

DETECTION OF KISSING BONDS IN FRICTION STIR WELDS

N.T. Sewell, Theta Technologies Limited, Exeter, UK
J.R. Wright, Theta Technologies Limited, Exeter, UK
J.C.S. Wright, Theta Technologies Limited, Exeter, UK

SYNOPSIS

This paper reports on the use of scanning non-linear acoustic NDT to detect the presence of kissing bonds in friction stir welded aluminium.

A pitch-catch head assembly was developed and mounted to a motorised scanner capable of scanning flat welds. A swept-frequency Pulse Inversion technique was applied to friction stir welded test pieces which had been specially fabricated to contain a range of kissing bond defects. Bespoke processing and graphical front-end software was developed to enable control of the scanning system and interpretation of the results from investigation of the scan data. This included the creation of a batch processing system for analysing many scans together and a number of visualisation tools with options to enable rapid analysis and interpretation of complex scan data.

The non-linear component of the response provides a quantification of defect levels in the test pieces. A low level of non-linear response was found when a known good weld was inspected, but there was a significant increase in the level of non-linearity when inspecting a weld known to contain defects.

To validate the non-linear inspection technique, three coupons from areas of interest identified from the scanning work were extracted from the original welded plate. Independent destructive investigation using optical and scanning electron microscopy demonstrated that the level of micro-cracking and kissing bonds present within the three samples showed a good correlation with the detected levels of non-linear response obtained from the scanning. The scale of defects detectable are of the order of 1µm wide by tens to hundreds of microns long.

INTRODUCTION

Theta Technologies have developed and tested a Friction Stir Weld (FSW) scanner comprising a contact based pitch-catch transducer head assembly and an automatically driven X-Y scanner for the inspection of flat friction stir welded plates (Sewell, 2015). Within the head, a transmitter and receiver are mounted on Rexolite wedges so that transmitted signals may interact with the welded section of a plate and may be picked up by the receiver as illustrated in Figure 1.

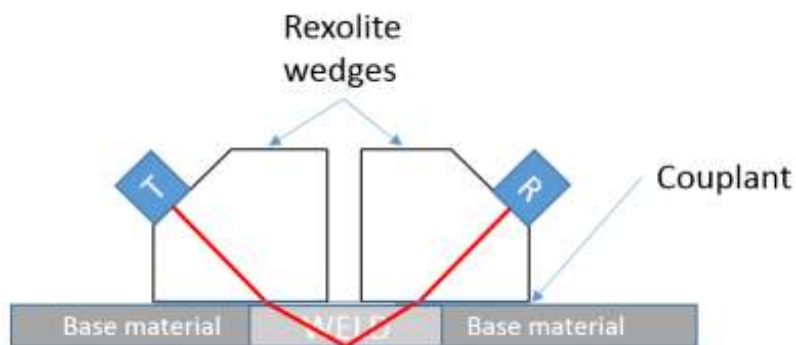


Figure 1 – The pitch-catch head assembly where T is the transmitter and R is the receiver.

The scanning system allows for samples to be mounted such that they may be scanned in the X-Y plane. Couplant is applied to the scan area and the scanning head traverses the area in steps deemed appropriate to the type of defect or damage sought. At each step the scanner emits a swept-frequency stimulus and its inverted complement which, when summed after reception, predominantly cancel to leave just the difference between the two. This is referred to as the residual. The residual time domain signal is converted to the frequency domain and this spectral representation is used to produce a graphical representation of the data at each scan position. A series of spectra are combined to form a *Thetagram*. Thetagrams show spectra from each scan position in one chart and provide a considerable quantity of information in a graphical form. They are a powerful way of examining the whole scan at a glance but can be hard for inexperienced operators to understand, so simpler views such as the “damage index” can also be shown. These charts are available in real-time as the scan proceeds.

The FSW scanner developed by Theta and used for this paper was designed to identify potential defects in aluminium alloy friction stir welds, specifically small or micro-defects such as kissing bonds where evidence exists of the reduction of strength and fatigue life of the part (Oosterkamp, 2004) (Kadlec, 2014)

The sample used for this investigation was provided by TWI, inventors of the FSW process, and contained an anticipated variable quality weld likely to contain kissing bonds. However, no other NDT technique was able to confirm this prior to the investigation so post-scanning, a destructive testing and subsequent validation process was performed by Theta. Previous work (Tabatabeipou, 2015) showed an apparent detection of a kissing bond but did not make reference to the base material or a known good weld and performed no validation under destructive investigation. These shortcomings were addressed by this and our previous work (Sewell, 2015).

This paper presents the work that we have undertaken to enhance the state of the art in FSW kissing bond defect detection, including the hardware and software development. The technology development is tested and non-linear NDT results are shown. They are validated using coupons taken from the scan area and inspected using both optical and scanning electron microscopy (SEM). A correlation between the non-linear response and the defect quantity is presented.

INVESTIGATION

The non-linear pulse inversion technique used in the work has been shown to be a powerful method for identifying material based non-linearities (Wright, 2013). Two discrete ultrasonic pulses, one the phase inverted version of the other, are injected into the sample and the captured responses are summed. Non-linear behaviour exhibited by the system manifests itself in the presence of even harmonics in the residual, i.e. a non-zero response from the summed received signals (Ma, 2005).

Critical to the repeatability and reproducibility of the results obtained using the FSW scanner has been the development of a novel head system capable of maintaining contact with the FSW surface whilst scanning. The pitch-catch assembly outlined in Figure 1 is mounted inside a bespoke manufactured housing to enable the independent movement of each of the Rexolite blocks whilst maintaining perpendicularity to the surface. The head system (shown in Figure 2) is adjustable to allow for different thickness plates and can be slid up or down and locked into position so that only a small amount of travel of the wedges is possible. The head is driven to each scan location using a dedicated motor controller and screw assembly, giving very low backlash and highly accurate repositioning. The motor control interacts with the controlling PC which synchronises the ultrasonic pulse emission and collection. This allows for a different resolution of scan to be undertaken depending on the type of defect sought and the speed at which the user wishes to inspect the sample.

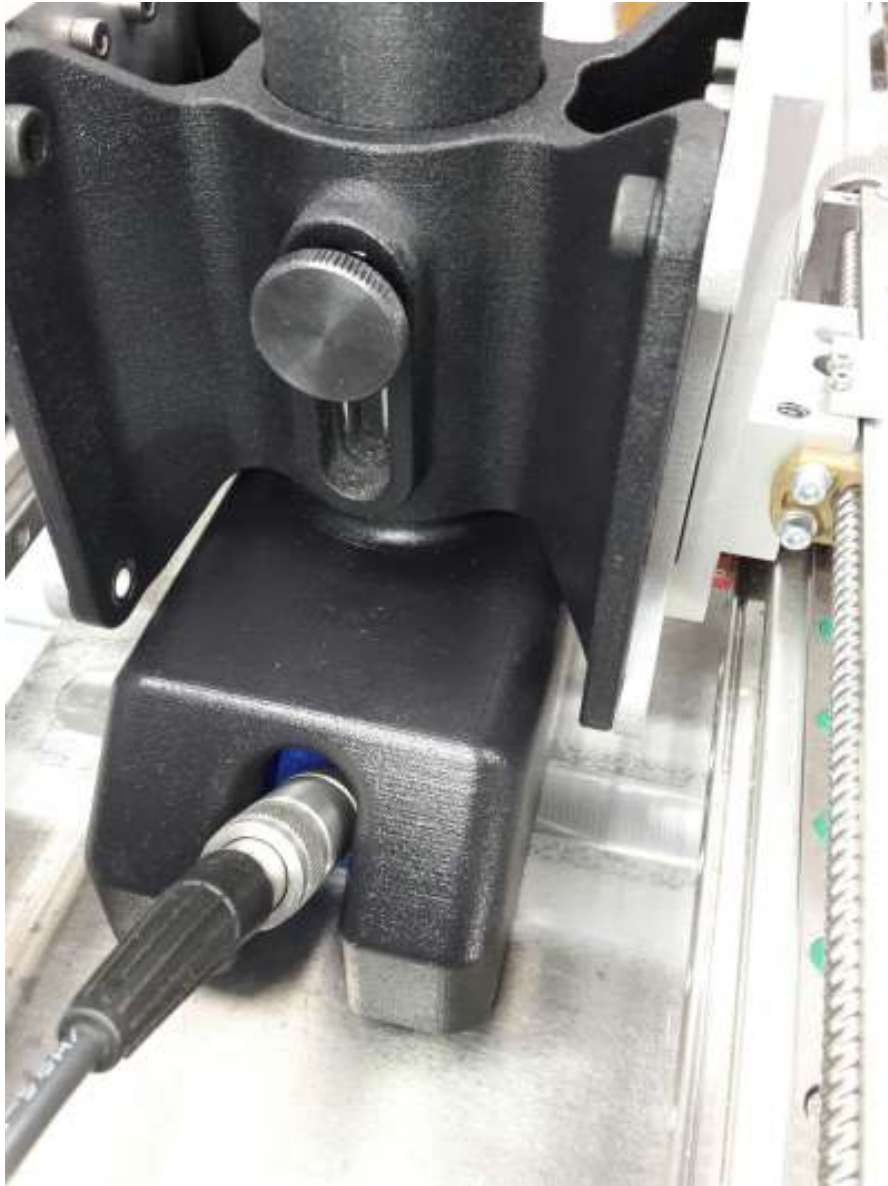


Figure 2 – Adjustable pitch-catch head system allows for varying thickness of plates

In addition to the hardware development, we have created software to make scanning easy and to make interpretation of results straightforward. The interactive system has three main screens of interest: The Inspection screen, the Data Map screen and the Analysis screen.

The Inspection screen allows the user to configure a scan and to execute the scan multiple times. Many of the scan parameters can be varied to make the system flexible to suit the scanning requirements. Once the scan is configured the user starts the scan and moves to the Data Map screen which shows the results in real-time.

The Data Map screen shows the Thetagram of the scan as the time domain response are received. The map builds up as the scan proceeds. Often, experienced users use this screen to monitor the system but novice users more often switch to the Analysis screen where the Damage Index is displayed.

The Damage Index is an indication of the level of non-linear response where a higher number is indicative of a greater degree of defect.

In this inspection a sample was provided by TWI which was believed to contain a kissing bond defect in a FSW of a 6mm thick, 2000 series aluminium alloy plate along at least part of the weld length. The sample was 500mm long by 300mm wide, with a 25mm wide weld zone running up the centre.

RESULTS

Figure 3 shows a Thetagram created whilst scanning the specially manufactured kissing bond sample. The Y-axis is the test position, in this case each millimetre of the scan, and the X-axis is the frequency. The residual obtained from each position in the scan is used to create a spectrum which is plotted in this Thetagram. The colour scale goes from blue, through greens, yellows, oranges and up into red, thus low values of non-linearity are blue and high values are red.

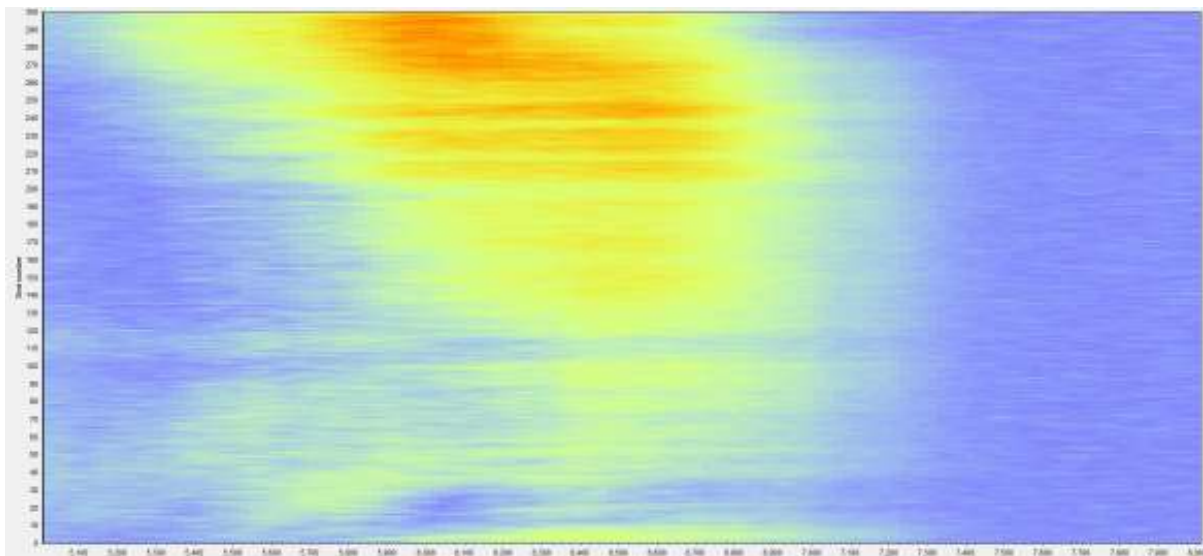


Figure 3 – Thetagram of sample plate

In Figure 3 it can be seen that the level of non-linear content increases from the bottom of the image towards the top. The bottom of the image relates to the beginning of the plate and the top relates to the end.

To an experienced user, the Thetagram is a useful visualisation as it shows both frequency and distribution of non-linear content, or indeed lack of it. However, it is a difficult view for inexperienced users to interpret and so the Damage Index is often used to simplify the feedback regarding the quality of the weld. The Damage Index graph for this scan is shown in Figure 4. It can be seen that for the first 100mm of the scan the Damage Index is very similar, varying by only 1 or 2dB, but after 120mm the damage index gradually ramps up.



Figure 4 – The Damage Index shows how the non-linear response changes over the scan.

Both figures show changes in the response for the FSW sample. In Figure 3 the Thetagram can be seen to be getting “hotter” in the area of the second harmonic and in Figure 4 the Damage Index can be seen to increase as the scan progresses. Several repeat scans were made of the plate and each produced similar results. These results were used to select the position of the coupons which were extracted and subsequently inspected using both visual and scanning electron microscopy.

The samples were cut from positions at 45mm from the start of the scan, 245mm from the start of the scan and 380mm from the start of the scan. They are referred to as Sample 1, Sample 2 and Sample 3 respectively.

Sample 1 was taken from the zone at the beginning of the scan which exhibited a low Damage Index. This sample was taken to identify how “low” correlated to the degree of damage that could be identified. Sample 2 was taken from an area where the Damage Index had been increasing steadily for some time but had not peaked, and where the Thetagram showed some consistent orange and red. Sample 3 was taken from the very end of the plate where there was greatest non-linearity and where the Damage Index reached a peak.

Each of the samples was removed from the sample by drilling a 2mm hole through the base material to the edge of the area of interest and using a wire cutting machine to remove a piece 30mm long by 10mm wide by 6mm deep from the plate. Although removing the samples from the panel is clearly a destructive technique, this method caused very little damage to the sample and was performed so that the plate could be scanned again after removal if required. Figure 5 shows the three samples removed from the plate.

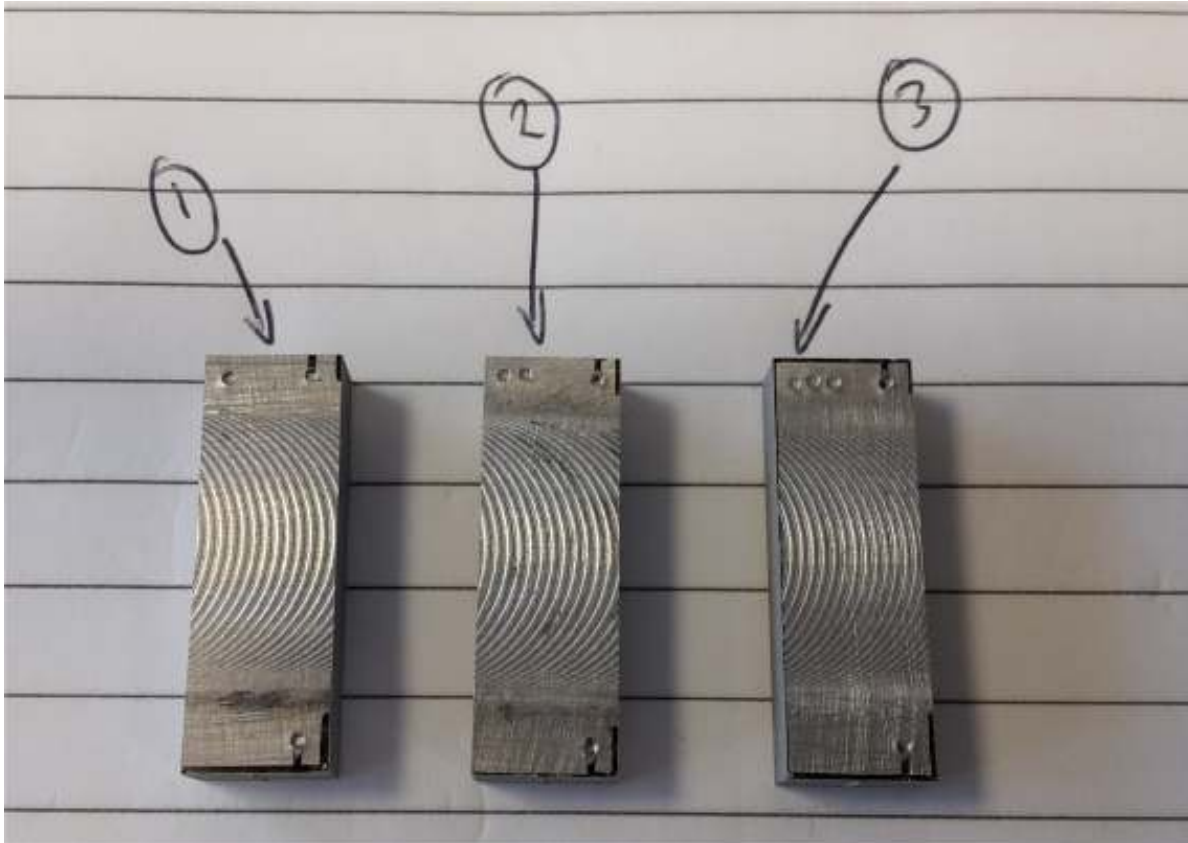


Figure 5 – The three samples cut from the manufactured defective plate

The three FSW coupons were cast separately in Stuers Epofix which was poured around them in a 40mm Leco plastic mould cup and then allowed to harden fully before being ground and polished such that the coupons were suitable for microscopy.

Optical Microscopy

Optical microscopy was undertaken using an Olympus U-TV0.5xC-3 camera. Close inspection of the weld at x100 magnification was used to produce the following figures in which the micro-cracks can be seen.

Figure 6 shows the centre section of the bottom of the weld taken from Sample 1 where the low level of non-linearity had been recorded. It can be seen from the figure that there are a few very small cracks present but that most of the image is crack free. A method of identifying the scale of these cracks was used and by area, this sample was deemed to have 15 micro-cracks per square millimetre, or approximately 0.15% crack by area.

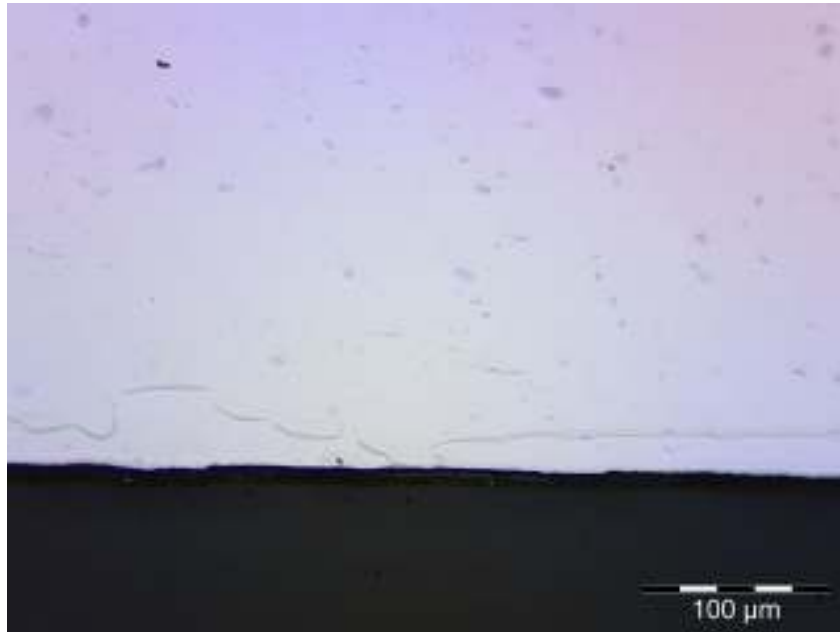


Figure 6 – Centre section of Sample 1, taken from the area of low harmonic response.

Figure 7 shows the centre section of the bottom of the weld taken from Sample 2 where the level of non-linearity had been increasing for some time but where it had not yet peaked. In this case, using the same method for approximating the degree of defect in the samples, it can be estimated that 35 micro-cracks are present per square mm, or 0.35% by area.

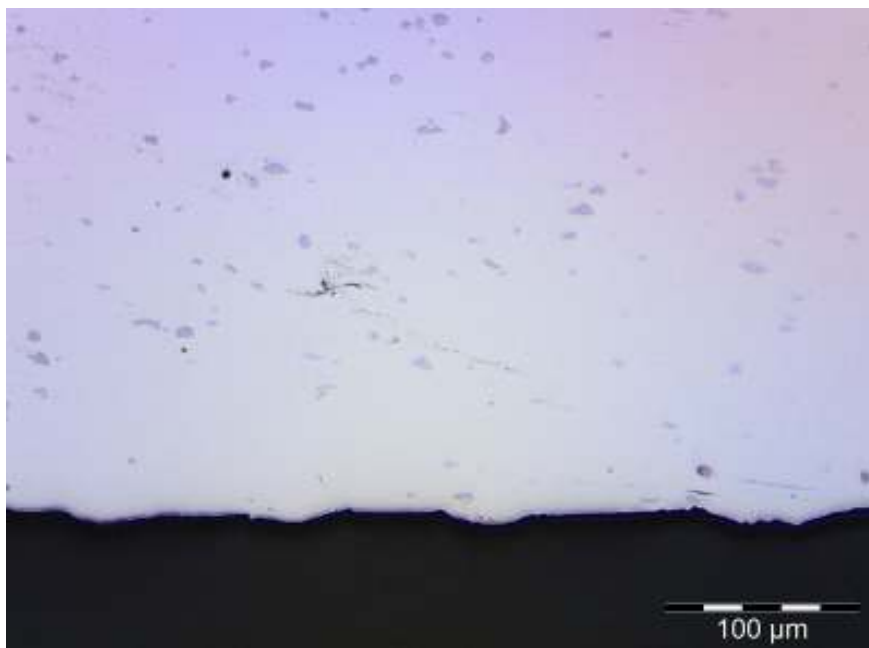


Figure 7 – Centre section of Sample 2, where the harmonic response was increasing.

Figure 8 shows the centre section of the bottom of the weld taken from Sample 3 where the highest level of non-linear response had been found. The same counting technique was used to assess the degree of damage in the sample and 150 micro-cracks per square mm were counted, representing 1.5% by area.

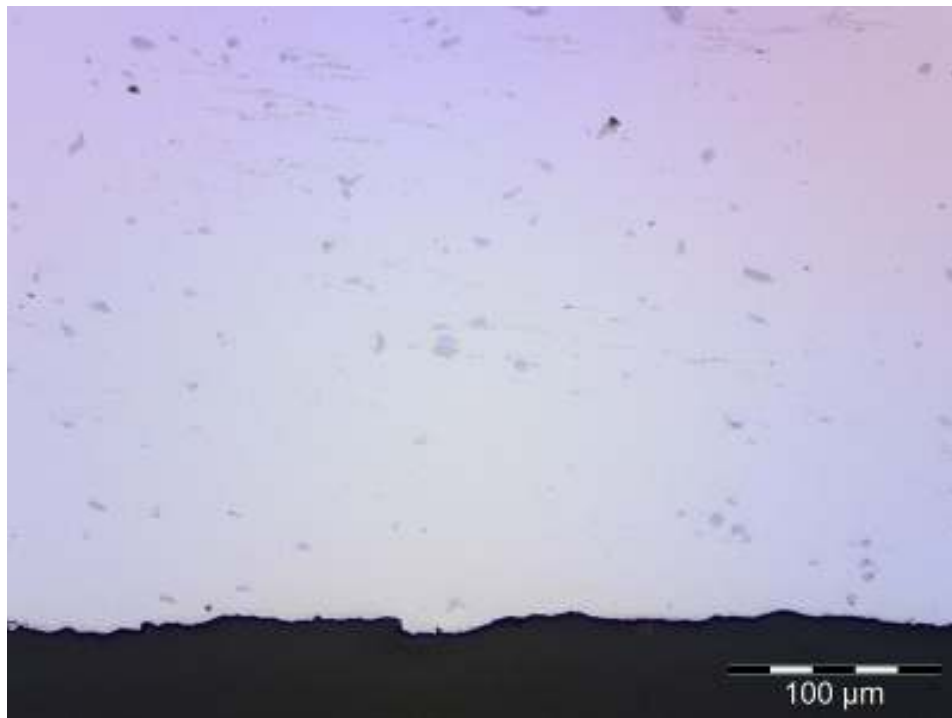


Figure 8 – Centre section of Sample 3 where the harmonic response was at its highest.

A control value was taken by inspecting the parent material to one side of the weld where it was observed that there were consistently approximately 7 micro-cracks per square millimetre, representing a background value of about 0.07% by area.

Table 1 – Results of the number of micro-cracks observed in the optical microscopy of the three extracted samples and in the parent material, the proportion of the area they represent and the damage index recorded at that point.

Sample	Number of micro-cracks	Area of micro-cracks (sq millimetre)	Proportion	Damage Index
1	2	0.0015	0.15%	4
2	5	0.0035	0.35%	14
3	20	0.015	1.50%	40
Parent Material	0	0.0007	0.01%	N/A (0)

SEM results

To further investigate how the degree of non-linearity is affected by the number and scale of the defects within the sample, the most non-linear sample, Sample 3, was inspected using SEM. The initial inspection was performed at x500 magnification in the area towards the bottom centre of the weld, just as for the optical microscopy. Here, numerous micro-cracks could be seen. Figure 9 shows the SEM image of Sample 3 at x500 magnification.

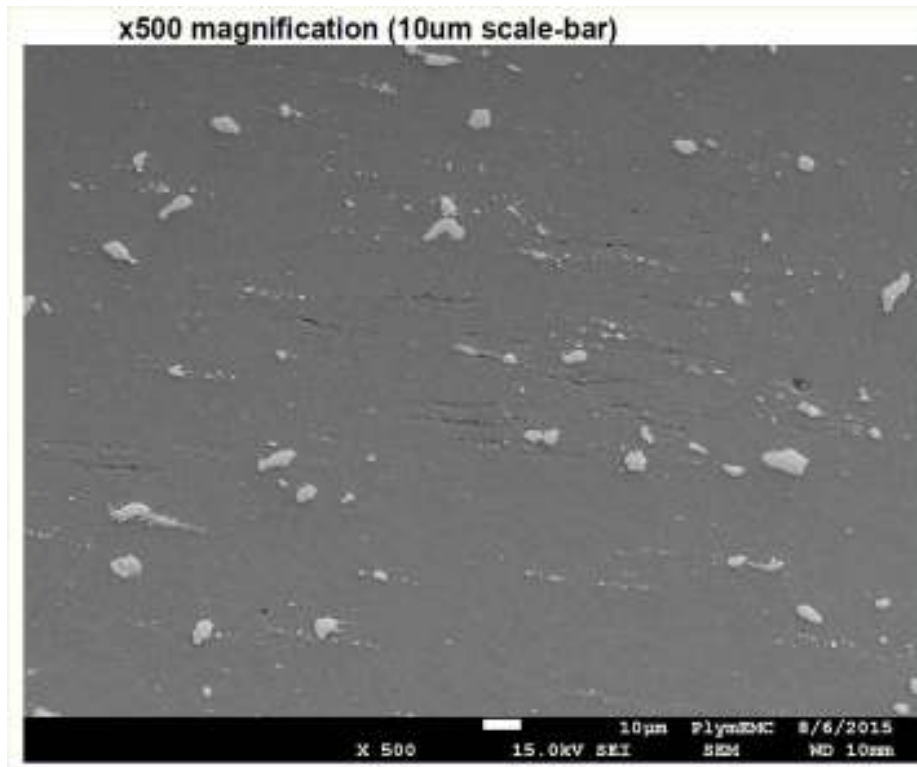


Figure 9 – SEM of Sample 3 at x500 magnification shows numerous micro-cracks.

By examining the part at higher magnification, the length and quantity of the micro-cracks can be seen more clearly, as shown in Figure 10.

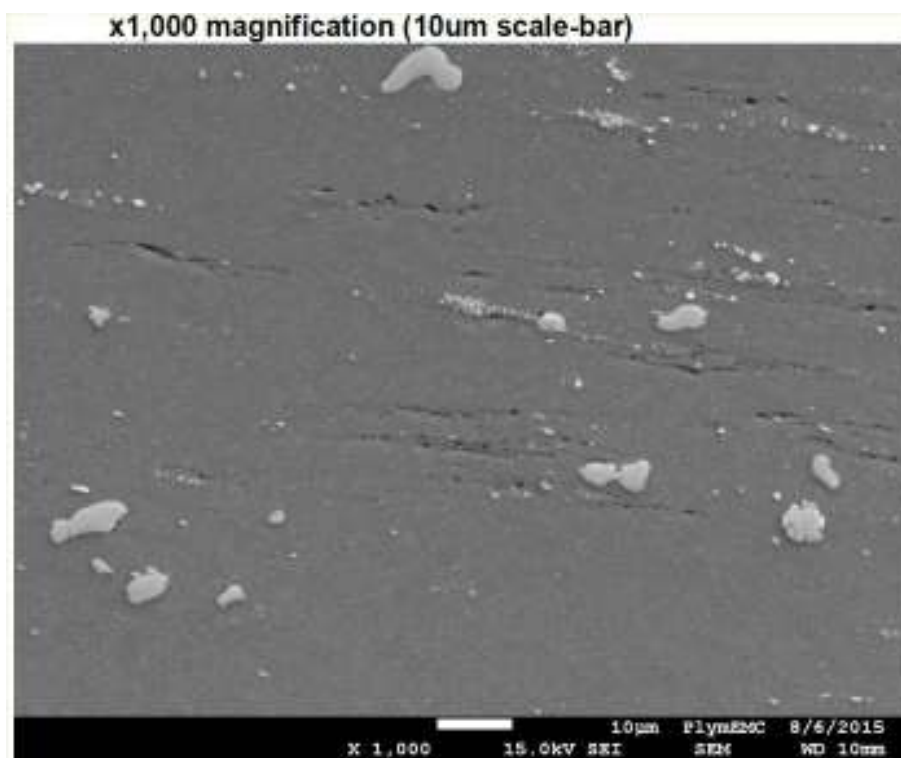


Figure 10 – SEM of Sample 3 at x1000 magnification. Cracks from tens to hundreds of microns long can be seen.

x3,500 magnification (1um scale-bar)

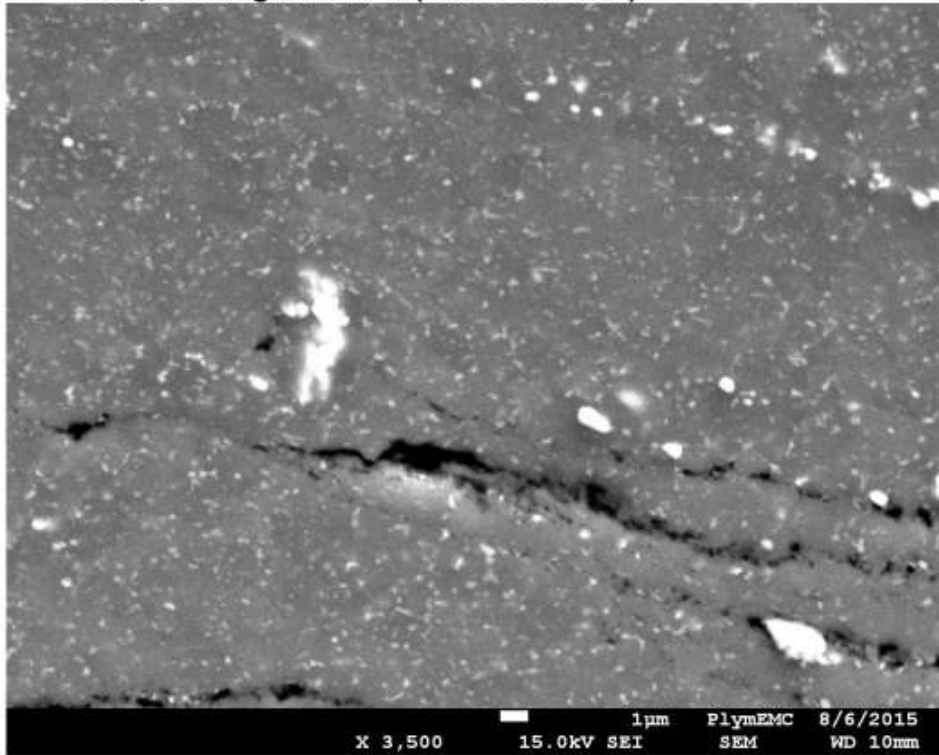


Figure 11 – SEM of Sample 3 at x3500 magnification shows that cracks are around 1um wide.

Figure 11 shows an SEM view of Sample 3 where micro-cracks of around 1um wide can be seen. These images show that the cracks measured under optical microscopy are kissing bonds.

Using the results from the optical microscopy and the SEM confirmation that the micro-cracks observed are kissing bonds it is possible to produce the graph in Figure 12 showing how the damage per unit area varies with the Damage Index measured during scanning. The graph shows that there is an approximate linear correlation between the damage index and the proportion of damaged material per unit area. This suggests that non-linear NDT can be used to identify kissing bonds in FSW.

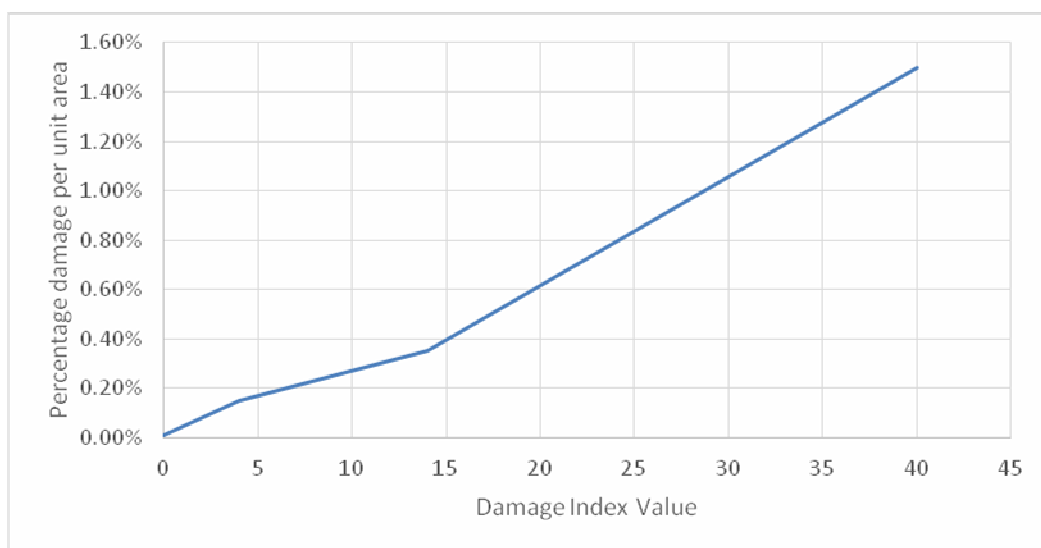


Figure 12 – Percentage of damage per unit area against Damage Index shows an approximately linear relation

CONCLUSIONS

This paper has presented the use of a non-linear acoustic NDT technique to inspect a FSW plate containing kissing bonds. Samples were removed from the plate, were mounted and polished and then inspected using both optical and SEM. The optical microscopy was used to identify micro-cracks which were present in all samples. No cracks were visible in the parent material. SEM was used to show that many of the micro-cracks were of the order of 1µm wide by tens or hundreds of microns long. The level of micro-crack correlated with the measured damage index value such that a relationship between the two can be seen to be approximately linear. This suggests that the level of kissing bond present in a FSW can be assessed by the Damage Index value calculated from non-linear scans of such welds.

ACKNOWLEDGEMENTS

We would like to thank TWI for the manufacture of the sample plate and the Plymouth Electron Microscopy Centre for both the optical and SEM inspections undertaken.

REFERENCES

- Kadlec M., Ružek, R., Nováková, L., Nor, K., Perrier, F., Nguyen-Dinh, A., Chatzakos, P.** Influence of the Kissing Bond Defect to the Fatigue Life in Friction Stir Welds of AA7475-T7351 Aluminium Alloy [Conference]. - Beijing : 10th International Symposium on Friction Stir Welding, 2014.
- Ma Q., Ma, Y., Gong, X., Zhang, D.** Improvement of tissue harmonic imaging using the pulse-inversion technique [Journal] // *Ultrasound in Medicine and Biology*. - 2005. - 7 : Vol. 31. - pp. 889–894.
- Mattei C.** Health monitoring of aircraft by nonlinear elastic wave spectroscopy [Report]. - [s.l.] : AERONEWS deliverable D3, EC sixth framework AT3-CT-2003-502927, 2008.
- Morris W.L., Buck, O., Inman, R.V.** Acoustic harmonic generation due to fatigue damage in high-strength aluminium [Journal] // *Journal of Applied Physics*. - 1979. - 11 : Vol. 50. - pp. 6737-6741.
- Oosterkamp A., Oosterkamp, L.D., Nordeide, A.** Kissing bond phenomena in solid-state welds of aluminium alloys [Journal]. - [s.l.] : *Welding Journal*, 2004. - 83. - pp. 225-231.
- Sewell N.T., Wright, J.C.S., Wright, J.R., Mottram, T.D.** Automated non-linear acoustic NDT of Friction Stir Welds [Conference] // *British Institute of NDT Conference*. - Telford : British Institute of NDT, 2015.
- Tabatabeipou M, Hettler, J, Delrue, S, Van den Abeele, K.** Nonlinear Ultrasonic Inspection of Friction Stir Welds [Conference]. - Brussels, Belgium : *Emerging Technologies in Non Destructive Testing 6*, 2015.
- Wright J.R., Armitage, P.R., Mottram, T.D.** Non-linear acoustics techniques for NDT [Conference]. - Telford : *British Institute of NDT Conference*, 2013.